Journal of the Korean Physical Society (2022) 81:1004–1012
https://doi.org/10.1007/s40042-022-00619-3

Online ISSN 1976-8524
Print ISSN 0374-4884

ORIGINAL PAPER - CROSS-DISCIPLINARY PHYSICS AND RELATED AREAS OF SCIENCE AND TECHNOLOGY

Absorbed dose to water standard of high-energy x-rays at the KRISS

In Jung Kim[1,2] · **Yun Ho Kim**[1] · **Chul-Young Yi**[1]

Received: 23 June 2022 / Revised: 16 August 2022 / Accepted: 7 September 2022 / Published online: 4 October 2022
© The Korean Physical Society 2022

Abstract
The Korea Research Institute of Standards and Science (KRISS) established the standard of absorbed dose to water of high-energy x-rays based on the graphite calorimetry. Some of the ionization chambers were directly calibrated under high-energy x-rays. Uncertainty of the chamber calibration was 0.43% ($k=1$). $k_{Q,Q0}$, the beam quality correction factor, of the chambers were determined for the chamber models of the NE2571 and PTW30013, too. Determined $k_{Q,Q0}$ showed good agreement with the literal data within the stated uncertainty. International equivalence of this KRISS standard was also confirmed, in separate studies, by participating in international comparison studies with the National Metrology Institute of Japan and also with the Bureau international des poids et mesures (BIPM.RI(I)-K6). Now, the KRISS is providing a direct calibration service for user's ionization chambers under high-energy x-rays. This service could contribute improving the quality assurance of x-ray therapy at hospitals by reducing the uncertainty of dose measurement.

Keywords Absorbed dose to water · Graphite calorimetry · Direct calibration · Beam quality correction factor

1 Introduction

The Korea Research Institute of Standards and Science (KRISS) established the standard of the absorbed dose to water for therapeutic high-energy x-rays and developed the direct calibration procedure for the ionization chambers under the high-energy x-rays. So far, the absorbed dose to water of high-energy x-rays used in domestic hospitals has been traceable to the absorbed dose to water of ^{60}Co gamma-rays standard of the Korea Research Institute of Standards and Science. The effect of the difference in quality between the high-energy x-rays and ^{60}Co gamma-rays is considered by using a quality correction factor, $k_{Q,Q0}$ (or k_Q) provided by IAEA Technical Report TRS-398 [1], an international protocol for external beam radiotherapy, or by TG-51 [2, 3] of the American Association of Medical Physicists. However, the $k_{Q,Q0}$ given in the protocol are provided only for each model of the chamber, so the characteristic difference between the chambers cannot be considered. This difference contributes to an increase in the uncertainty of the absorbed dose to water, which affects the quality control of the radiation therapy. For this reason, direct calibration under high-energy x-rays has been carried out in the UK since 1989 [4, 5] (direct calibration of the air kerma until the 1990s). Recently, direct calibration of water absorbed dose for high-energy x-rays has been mandatory in Australia since 2014 [6]. In Korea, all technical preparations for direct calibration has already been completed at KRISS.

Measurement traceability is a characteristic that connects the measurement results to measurement standards through an unbroken chain of the calibration [7]. Measurement traceability enables the comparison of results measured by different equipment or people at different times, places or hospitals. In other words, the measurement results are equivalent within a range of the combined uncertainty. This is the core of the quality assurance of treatment, which allows treatment policies to be maintained consistent and makes it possible to accumulate case experiences in each hospital, and to compare and share the treatment results among the radiation oncologists working in different hospitals [8].

One of the most important elements in the measurement traceability is the uncertainty. It is because the uncertainty allows the measurement results to be compared with each

✉ In Jung Kim
kimij@kriss.re.kr

[1] Korea Research Institute of Standards and Science, Daejeon 34113, Korea

[2] University of Science and Technology, Daejeon 34113, Korea

other. For this reason, until the early 2000s, countries around the world accepted the revised protocol which was shifted from the air kerma based [4, 9, 10] to the absorbed dose to water based [1–3, 5].

ICRU 24 requires the uncertainty of the absorbed dose to the target volume should be within 5% ($k=1$) [11]. And there is a need for lower uncertainty for radiation-sensitive tissues. However, it is not easy to maintain the uncertainty of the absorbed dose to the patient below 5% [12]. Of course, the major reason is that the dose in the patient's body is entirely dependent on calculation. However, the uncertainty involved in the calibration of high-energy x-rays cannot be ignored, yet. Following the standard protocols based on the current ^{60}Co gamma-rays absorbed dose standard, the expected uncertainty of the measured absorbed dose to water under the high-energy x-rays is typically about 1.5% ($k=1$) [1], where the uncertainty of 1% ($k=1$) is caused by $k_{Q,Q0}$ [1]. With the direct calibration in the high-energy x-rays, the uncertainty in the dose measurement can be reduced down to less than 1%. For this reason, TRS-398 recommends the direct calibration as the top priority if it is available.

Direct calibration under the high-energy x-rays has not yet become common, for several reasons. The first reason is the technical difficulty. The most preferred primary method of the measurement of absorbed dose to water under high-energy x-rays is calorimetry using water or graphite as a medium. The calorimetry was first developed in the 1970s by the National Bureau of Standards (NBS) [13]. However, due to the difficulty of implementing the technology, it did not spread until the 2000s. Currently, about ten countries have established their own standards for absorbed dose to water under the high-energy x-rays and maintaining their international equivalence of measurements through the CIPM Mutual Recognition Arrangement (CIPM MRA), where CIPM stands for International Committee for Weights and Measures (Comité international des poids et mesures). KRISS developed a graphite calorimeter in 2015 and conducted international comparison studies with National Metrology Institute of Japan (NMIJ) in 2016 [14] and with the International Bureau of Weights and Measures (Bureau international des poids et mesures, BIPM) in 2017 (BIPM. RI(I)-K6) to demonstrate the international equivalence of the new measurement standard. The degree of equivalence of the KRISS standard is maintained in the BIPM's key comparison database (KCDB) [15] at http://kcdb.bipm.org.

The second reason is the argument that the direct calibration is not necessary because the standard for absorbed dose to water under ^{60}Co gamma-rays is more consistent among countries than in the case of the high-energy x-rays [6]. This contributes solely to the superior stability of ^{60}Co gamma-rays. The ^{60}Co gamma-ray field simply decays with the half-life but the x-rays of an electron accelerator cannot be so constant. In fact, the international comparison results under ^{60}Co gamma-rays are relatively better; however, this is meaningless since the calibration under ^{60}Co gamma-rays eventually increases the uncertainty of the hospital users.

The third reason is the economic burden of the secondary standard dosimetry laboratory (SSDL). In order to fully implement direct calibration, the SSDLs have electronic linear accelerators incurring a lot of cost burden. This is an important issue because it may threaten current calibration system, and is also the main reason for not accepting direct calibration in North America. For this reason, TRS-398 suggests that it is not necessary to undergo direct calibration under high-energy x-rays every year and proposes to perform a direct calibration every third calibration cycle or when damage to the ionization chamber is suspected. However, recently, with the widespread use of the electron linear accelerators, some studies on the feasibility of direct calibration in the SSDL have been conducted [16, 17].

Direct calibration under high-energy x-rays can also be used for quality assurance purpose. As mentioned above, the $k_{Q,Q0}$ values provided by the protocol cannot cover the differences between the individual ion chambers. Even within the same model of chambers, the characteristics may differ due to the structural differences in production or metamorphosis during storage. In fact, in 2010, a study conducted in Korea reported a variation in response up to 2.4% within a same chamber model [18]. This is a much larger difference than the uncertainty (1%, $k=1$) of $k_{Q,Q0}$ suggested in the protocol and may degrade the treatment quality. This kind of problem can be found and be acted upon via an external audit as claimed by S.H. Kim et al. [18].

In this manuscript, the procedure of direct calibration established by the KRISS and the resulting $k_{Q,Q0}$ values obtained through measurement of some ion chambers are presented.

2 Materials and methods

2.1 Graphite calorimeter

Graphite calorimeter model C1505-4 was used [19]. The schematic structure of the model C1505-4 is as shown in Fig. 1, which was installed and operated as shown in Fig. 2.

Model C1505-4 is a Domen type calorimeter. The core has a diameter and thickness of 16 mm and 3 mm, respectively, equipped with three thermistor thermometers and one thermistor heater, and is covered with two layers of jackets. The temperature change in the core was measured by a DC-type Wheatstone bridge. The signal noise of the Wheatstone bridge is about 0.3 μVpp, which corresponds to a temperature of 0.08 mK. More details on the model C1505-4 are reported in Ref. [19].

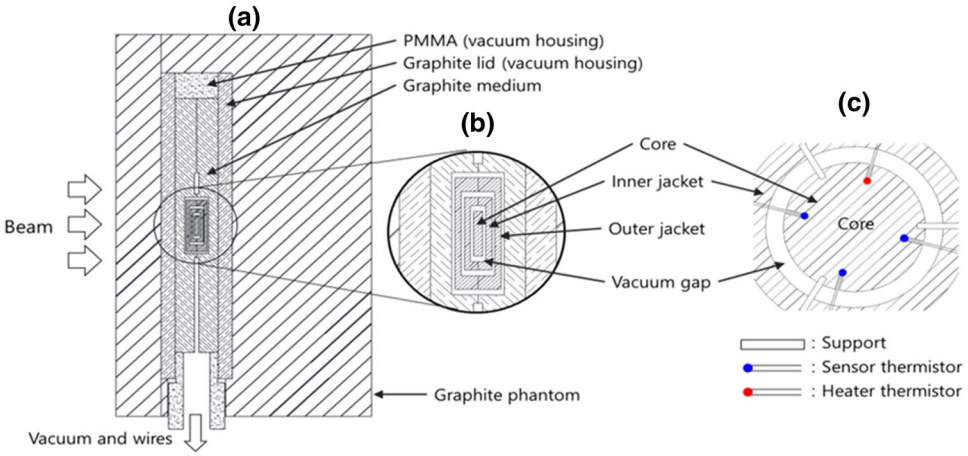

Fig. 1 Schematic of the graphite calorimeter model C1505-4. Cross-sectional layout (**a**), close-up of the core and jackets (**b**), and arrangement of the core thermistors (**c**)

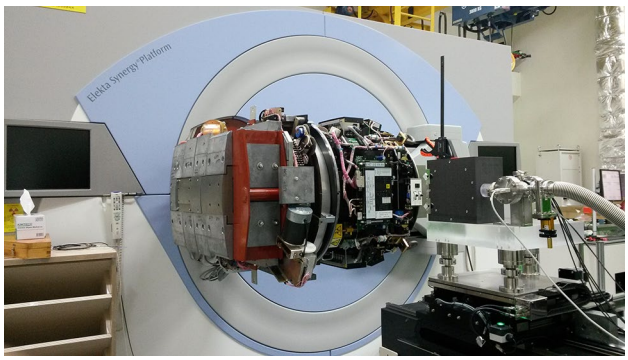

Fig. 2 Picture of the graphite calorimeter model C1505-4 set up

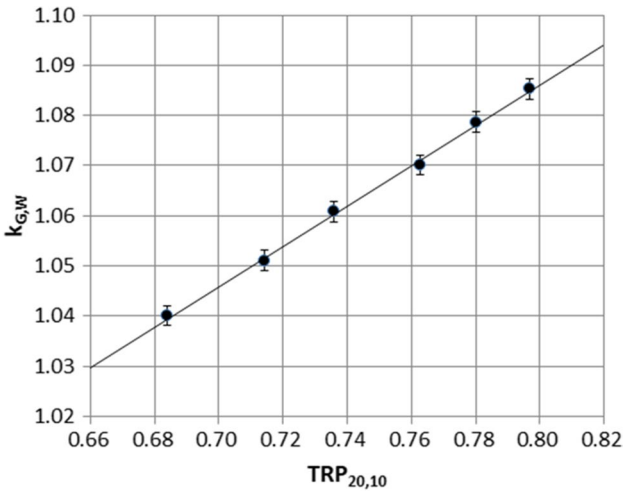

Fig. 3 Plot of the determined graphite-to-water conversion factor according to the beam quality index, $TPR_{20,10}$

From the signals of the graphite calorimeter core, the water absorbed dose was determined through two steps. First, the graphite absorbed dose was determined, and second, multiplied by the graphite-to-water absorbed dose conversion factor to finally determine the water absorbed dose.

In order to determine the graphite absorbed dose, it was necessary to know the energy of the radiation absorbed in the core and the mass of the core. The mass of the core was determined to be $(1.103\,47 \pm 0.000\,11)$ g through precise measurements when the graphite calorimeter was built. The radiation energy absorbed by the core was determined through an electric power calibration procedure, that is, a process of comparing the temperature rise of the core raised by radiation with the temperature rise of the core due to electric heating up by the thermistor heater. The power P_x supplied from the thermistor heater was determined as $P_x = V_x V_s / R_s$, where V_x, V_s were the voltage drops across the thermistor heater and a constant standard resistance (resistance value R_s) connected in series to the thermistor heater, respectively. Therefore, the graphite absorbed dose was traceable to the unit of absorbed dose (Gy) through the calibrations with the mass standard (kg), voltage standard (V), and resistance standard (Ω).

The graphite-to-water absorbed dose conversion factor, $k_{G,W}$, was determined using a Monte Carlo simulation technique [20]. This method was validated by previous research groups [21–23]. EGSnrc code [24] was used in this study. $k_{G,W}$ was determined as $k_{G,W} = D_W / D_G$, where D_W, D_G were the absorbed dose calculated at the calibration point (10 g/cm^2 water depth at the central axis of the beam) in a water phantom ($30 \times 30 \times 30$ cm^3) and at the core center of the computational model of the graphite calorimeter, respectively. $k_{G,W,}$ includes the gap effect correction [25] and the depth correction, as well. $k_{G,W}$ of the model C1505-4 thus determined was as shown in Fig. 3. Figure 3 shows the pattern of $k_{G,W}$ against the beam quality index of high-energy x-rays, i.e., tissue phantom ratio 20, 10 ($TPR_{20,10}$). Details of $k_{G,W}$ evaluation were reported in Ref. [20].

2.2 High-energy x-ray standard field

High-energy x-ray standard fields are generated using a medical linear electron accelerator model Elekta Synergy® Platform. Three types of x-ray energy sets (6, 10, 18) MV, (6, 10, 15) MV, (4, 8, 25) MV can be configured through combination of filters of the accelerator. (6, 10, 18) MV set has been the default since 2015. The reference irradiation direction of the x-rays was horizontal. All the irradiations in this study were performed in horizontal setting but the characterization of the x-rays. Characteristics of the x-rays were evaluated using a large water phantom ($50\times50\times40$ cm^3) in vertical setting to evaluate such as x-ray beam quality index ($TPR_{20,10}$), lateral profile, and percentage depth dose.

Accelerator x-rays are not such stable as the ^{60}Co gamma-rays. Thus, for the sake of calibrating ionization chambers against the water absorbed dose standard, precise monitoring of the x-rays was needed. To this end, an external monitor chamber was prepared with two thimble-shaped chambers (0.53 cc in volume) connected in parallel and placed after the x-ray emission window. A high-purity, high-density graphite cylinder (12.8 mm inner diameter and 25 mm outer diameter) was overlaid on the monitor chamber to obtain a sufficiently built-up signal. The two ionization chambers were 62.5 mm apart from the center of the beam along the cross-line direction. The ionization current was measured with a precision electrometer, and the temperature and pressure were also measured to correct the effect of air density. The installed external monitor chambers were as shown in Fig. 4. In the case of the medical accelerator of the KRISS, the stability of the inherent monitor chamber installed inside the accelerator was within 0.3% for a day or two, and the stability of the additionally mounted external monitor chambers was within 0.15%.

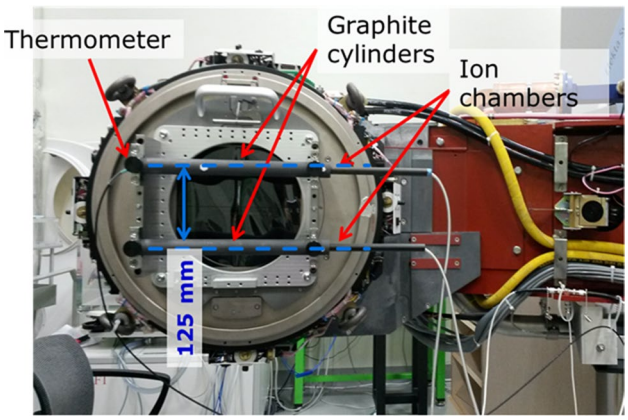

Fig. 4 Picture of the external monitor chamber(s) set up on the accelerator

2.3 Absolute measurement of water absorbed dose

Using the graphite calorimeter, the water absorption dose (rate) ($D_W/Q_{m,g}$) (Gy/nC) of the high-energy x-ray was determined as follows:

$$\left(\frac{D_W}{Q_{m,g}}\right)=\left(\frac{\Delta T_{irr}}{Q_{m,g}}\right)\left(\frac{C_{eff}}{m_{eff}}\right)\prod_{i=1}k_{i,g} \tag{1}$$

where $Q_{m,g}$ was the amount of charge (C) measured by the external monitor chamber, ΔT_{irr} was the temperature rise (K) of the core by irradiation, and C_{eff} was the effective heat capacity of the core (J/K) [19, 26, 27], m_{eff} was the effective mass of the core [19, 23, 27, 28], and $k_{i,g}$ were various correction factors including the graphite-to-water absorption dose conversion factor. C_{eff} (J/K) was decided as follows.

$$C_{eff}=\left(\frac{E_{E\_cal}}{\Delta T_{E\_cal}}\right)k_{heater} \tag{2}$$

where E_{E_cal} (J) was the electric energy (J) supplied to thermistor heater for electric power calibration, ΔT_{E_cal} (K) was the temperature rise (K) of the core by electric heating, and k_{heater} was a correction factor for the geometric difference between electric and radiation heating [29].

The calorimeter was positioned so that the center of the graphite calorimeter core was located at a source-to-chamber distance (SCD) of 100 cm. For electric power calibration, electric heating was performed before and after irradiations. Electric heat was supplied approximately at the same rate as the energy absorption expected under the irradiation.

2.4 Calibration of standard ionization chamber

In the high-energy x-ray standard field where the quality was Q, the calibration factors $N_{D,W,Q}$ of the standard ionization chamber was determined as follows.

$$N_{D,W,Q}=\left(\frac{D_W}{Q_{m,g}}\right)/\left(\frac{M_Q}{Q_{m,ch}}\right) \tag{3}$$

where M_Q was the amount of charge (C) measured by the standard ionization chamber and $Q_{m,ch}$ was the amount of charge (C) measured by the external monitor ionization chamber. M_Q was given as follows:

$$M_Q=M_{raw}k_s k_{pol}k_{nr,ch}k_{sleeve}k_{depth,ch}k_{SCD,ch} \tag{4}$$

where M_{raw} was the reading of the standard ionization chamber after the correction for the temperature and pressure was applied, k_s was the recombination correction factor, k_{pol} was the polarity effect correction factor, $k_{nr,ch}$ was the radial non-uniformity correction factor for the x-ray standard field, and k_{depth} was the water depth correction factor, k_{sleeve}, was the

Table 1 The ionization chambers used in this study

Model	Serial number	Chamber type	Nominal volume, cm^3	$N_{D,W,Q0}$, Gy/μC
PTW TN30013	8979	Farmer	0.60	53.59 ± 0.17
PTW TN30013	9304	Farmer	0.60	53.79 ± 0.20
PTW TN30013	9305	Farmer	0.60	53.73 ± 0.20
NE2571	3744	Farmer	0.60	44.95 ± 0.15
NE2571	3745	Farmer	0.60	45.12 ± 0.15

sleeve effect correction factor, and k_{SCD} was the SCD correction factor. The reference temperature and pressure were 20 ℃ and 101.325 kPa, respectively, when correcting the environmental factors of temperature and pressure.

Five farmer type chambers were calibrated against the graphite calorimeter. Table 1 shows the basic information of the chambers used for the measurement.

The chambers were irradiated in a waterproof sleeve in a water phantom (30 × 30 × 30 cm^3). The reference point of the chamber was the geometric center of the chamber, and the reference point was placed at a water depth of 10 g/cm^2 on the beam central axis. Since the irradiation direction was horizontal, the phantom window thickness (4.36 mm water equivalent) was included in the water depth. The sleeve was not necessary in the case of a waterproof chamber but had the advantage of improving the positioning reproducibility of the chamber during calibration. When measuring the ionization chamber, the laboratory temperature and humidity were maintained at in the range 20–24 ℃ and 30–70% of relative humidity, respectively, according to the KRISS calibration procedure.

The beam quality correction factors $k_{Q,Q0}$ of the chambers also were determined as follows from $N_{D,W,Q}$:

$$k_{Q,Q0} = \frac{N_{D,W,Q}}{N_{D,W,Q0}} \tag{5}$$

where $N_{D,W,Q0}$ was the calibration factor for the water absorbed dose of the corresponding ionization chamber in the standard ^{60}Co gamma-ray field.

2.5 Calibration of user ionization chambers

In this study, user ionization chamber calibration was not carried out. However, when a user chamber is submitted for calibration, then it is calibrated against the standard chambers in the same quality of x-rays in the same water phantom, in the same sleeve at the same location and at the same depth. And calibration factor of the user chamber $N^{user}_{D,W,Q}$ is determined as follows:

$$N^{user}_{D,W,Q} = \left(\frac{M_Q / Q_{m,ch}}{M^{user}_Q / Q^{user}_{m,ch}} \right) N_{D,W,Q} \tag{6}$$

Here, $N_{D,W,Q}$ is the calibration factors of the standard chamber, and M_Q, $Q_{m,ch}$ and M^{user}_Q, $Q^{user}_{m,ch}$ are the amount of the charges measured with the user chamber and the external monitor chamber, respectively, under the calibration.

3 Results and discussion

The typical temperature curve obtained with the graphite calorimeter was as shown in Fig. 5. It was obtained under the irradiation of 6 MV x-rays. Here, ΔT_{irr}, ΔT_{E_cal} was obtained by extrapolating the pre- and post-drift of

Table 2 Determined absorbed dose (rate) to water and the associated uncertainty at 10 MV ($TPR_{20,10}$ = 0.734)

	Value	Uncertainty	
		Type A (%)	Type B (%)
$(\Delta T_{irr}/Q_{m,g})$, core temperature rise (rate), K/μC	0.6323	0.05	0.06
C_{eff}, effective heat capacity of the core, J/K	0.8001	0.05	0.24
m_{eff}, effective mass of the core, g	1.1042	0	0.05
$k_{G,W}$, graphite-to-water conversion factor	1.0608	0	0.19
k_{BS}, backscattering to the monitor by the calorimeter	0.9997	0	0.05
$k_{rn,g}$, radial non-uniformity correction of the beam	0.9980	0	0.10
$k_{pos,g}$, correction for the lateral positioning	1	0	0.03
$k_{scd,g}$, correction for SCD	1	0	0.06
$(D_W/Q_{m,g})$, absorbed dose (rate) to water, Gy/nC	0.4849	0.07	0.34
u_{std}, standard uncertainty, Gy/nC	0.0013	0.35	

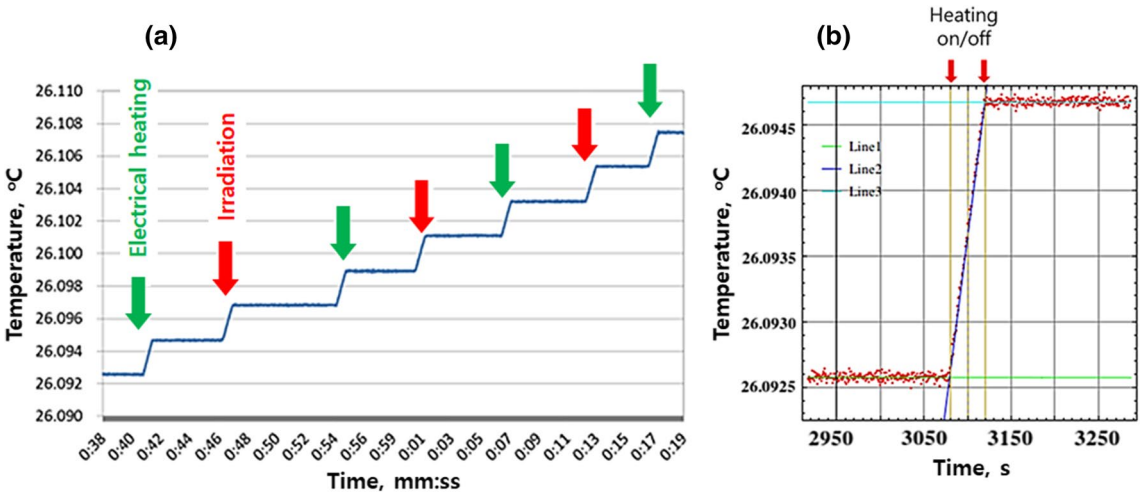

Fig. 5 Temperature rise of the core along the time (**a**), the temperature drift pre- and post-heating regions (**b**)

Table 3 Determined $N_{D,W,Q}$ of a farmer type chamber (PTW TN30013, SN9304) and the associated uncertainty at 10 MV ($TPR_{20,10}$ = 0.734)

	Value	Uncertainty	
		Type A (%)	Type B (%)
$(D_W/Q_{m,g})$, absorbed dose (rate) to water, Gy/nC	0.4849	0	0.35
$(M_{raw}/Q_{m,ch})$, ionized charge (rate) obtained, C/C	−9.167	0.02	0.06
k_s, recombination correction	1.0029	0	0.05
k_{pol}, polarity correction	−0.9997	0	0.04
$k_{nr,ch}$, radial non-uniformity correction of the beam	0.9980	0	0.15
k_{sleeve}, correction for the sleeve effect	1.0018	0	0.15
$k_{depth,ch}$, correction for the depth of water	1	0	0.05
$k_{scd,ch}$, correction for SCD	1	0	0.06
$N_{D,W,Q}$, calibration factor of the ion chamber, Gy/nC	0.5277	0.02	0.43
u_{std}, standard uncertainty, Gy/nC	0.0023	0.43	

Table 4 Experimentally determined $k_{Q,Q0}$ of the farmer type chambers

Beam energy	Beam quality		PTW TN30013		NE2571	
	$TPR_{20,10}$	$\%dd(10)_x$	$k_{Q,Q0}$	u_{std}	$k_{Q,Q0}$	u_{std}
6 MV	0.684	68.2	0.9884	0.0032	0.9905	0.0031
8 MV	0.714	71.3	0.9859	0.0032	–	–
10 MV	0.734	73.8	0.9798	0.0032	0.9833	0.0031
15 MV	0.766	78.6	0.9723	0.0032	–	–
18 MV	0.778	80.9	0.9684	0.0032	0.9715	0.0031
25 MV	0.799	85.2	0.9582	0.0036	–	–

the temperature to the midpoint of the heating [30, 31] as shown in Fig. 5b.

Using Eq. (1), the water absorbed dose (rate) of the x-rays was determined as shown in Table 2, which is given as an example of the absolute measurement results of water absorbed dose (rate) at 10 MV x-rays. The relative standard uncertainty of the determined water absorbed dose (rate) was about 0.26%, and the uncertainty due to statistical nature was small, 0.07%. Most of the type B uncertainty originated from the measurement of the effective heat capacity and the determination of the graphite-to-water conversion factor.

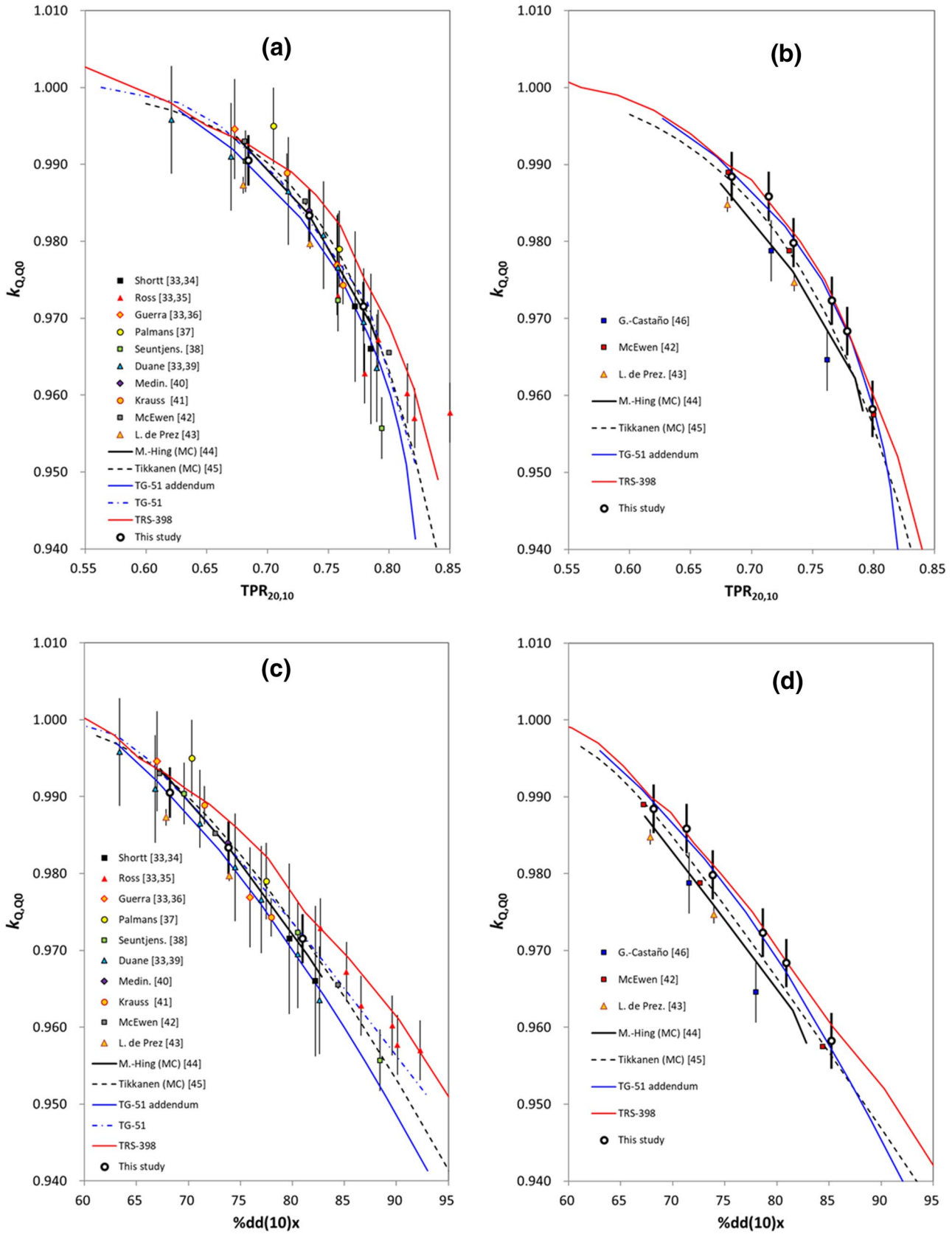

Fig. 6 Plot of $k_{Q,Q0}$ from this study and the literature. **a**, **c** for the NE2571 chamber against the beam quality index $TPR_{20,10}$ and $\%dd(10)_x$. **b**, **d** for the PTW TN30013 chamber against the beam quality index $TPR_{20,10}$ and $\%dd(10)_x$

Using Eqs. (3) and (4), the calibration coefficient for the water absorbed dose of the standard ionization chamber were determined as shown in Table 3 where the calibration results of the PTW TN30013 (SN9304) ionization chamber at 10 MV are given.

Tables 4 shows $k_{Q,Q0}$ for each model of the PTW TN30013 and NE2571 chambers determined from the measurements. In Fig. 6, the quality factor is shown as a function of $TPR_{20,10}$ and $\%dd(10)_x$. $\%dd(10)_x$ was converted from the measured $TPR_{20,10}$ according to the empirical formula of N. I. Kalach and D. W. O. Rogers [32]. It can be seen that the tendency for the quality of $k_{Q,Q0}$ is close to linear when the quality factor is plotted along $\%dd(10)_x$ [33].

$k_{Q,Q0}$ determined in this study agreed well with the values obtained by other groups. It is expected that the chambers being used in domestic hospitals could be confirmed their $k_{Q,Q0}$ values.

4 Conclusion

The KRISS established the standard for absorbed dose to water of high-energy x-rays with the standard uncertainty of 0.35% ($k=1$) using the graphite calorimetry. The degree of equivalence of the KRISS standard was also confirmed, although it was conducted in a separate study, it is still accessible via the BIPM's key comparison database (KCDB) [15] at http://kcdb.bipm.org. Now, the KRISS is providing a calibration service for user's ionization chambers.

The KRISS also has established direct calibration procedure of ionization chambers against the new standard. In this study, some ionization chambers have been calibrated and their calibration coefficients were determined with a small standard uncertainty at 0.43% ($k=1$). $k_{Q,Q0}$, the beam quality correction factor, of the ionization chambers were also obtained, and they were in good agreement with the values reported in the existing literature within the stated uncertainty.

Now, the KRISS is ready to disseminate their high-energy x-ray water absorbed dose standard to users and providing direct calibration services. The calibration uncertainty of user's chamber would be 0.5% ($k=1$). This uncertainty is small enough to reduce the uncertainty of the absolute dose measurement of user x-rays down to 1% or less ($k=1$). These services would contribute to improving the quality of x-ray treatment in hospitals by reducing the uncertainty in dosimetry.

Acknowledgements This work was supported by the Korea Research Institute of Standards and Science, Rep. of Korea under the project 'Development of measurement standards for ionizing radiation' with the grant number 19011053.

References

1. IAEA, Absorbed dose determination in external beam radiotherapy: an international code of practice for dosimetry based on standards of absorbed dose to water, TRS 398, Vienna, 2000.
2. P.R. Almond, P.J. Biggs, B.M. Coursey, W.F. Hanson, M.S. Huq, R. Nath, D.W.O. Rogers, AAPM's TG-51 protocol for clinical reference dosimetry of high-energy photon and electron beams. Med. Phys. **26**, 1847–1870 (1999)
3. M. McEwen, L. DeWerd, G. Ibbott, D. Followill, D.W.O. Rogers, S. Seltzer, J. Seuntjens, Addendum to the AAPM's TG-51 protocol for clinical reference dosimetry of high-energy photon beams. Med. Phys. **41**, 04150-1–04150-20 (2014)
4. S.C. Lillicrap, J.E. Burns, D. Greene, P.C. Williams, Revised code of practice for the dosimetry of 2 to 35 V x-rays and of caesium-137 and cobalt-60 γ-ray beams. Phys. Med. Biol. **28**, 1097–104 (1983)
5. S.C. Lillicrap, B. Owen, J.R. Williams, P.C. Williams, Code of practice for high-energy photon therapy dosimetry based on the NPL absorbed dose calibration service. Phys. Med. Biol. **35**, 1355–1360 (1990)
6. D.J. Butler, G. Ramanathan, C. Oliver, A. Cole, J. Lye, P.D. Harty, T. Wright, D.V. Webb, D.S. Followill, Direct megavoltage photon calibration service in Australia. Australas Phys. Eng. Sci. Med. **37**, 753–761 (2014)
7. International Vocabulary of Metrology – Basic and General Concepts and Associated Terms (VIM 3rd edition), JCGM 200:2012 (JCGM 200:2008 with minor corrections)
8. ICRU, Prescribing, Recording, and Reporting Photon Beam Therapy, ICRU Report No. 50, MD, 1993
9. IAEA, Absorbed dose determination in Photon and Electron Beams, An International code of Practice, TRS 277, Vienna, 1987.
10. Task Group 21, A protocol for the determination of absorbed dose from high-energy photon and electron beams. Med. Phys. **10**, 741–771 (1983)
11. ICRU, Determination of absorbed dose in a patient irradiated by beams of X or gamma rays in radiotherapy procedures, ICRU Report No. 24, MD, 1976.
12. ICRP, Prevention of Accidents to Patients Undergoing Radiation Therapy, ICRP Publication 86. Ann. ICRP 30 (3), 2000.
13. S.R. Domen, A heat-loss-compensated calorimeter and related theorems. J. Res. Natl. Bur. Stand. **73C**, 17–20 (1969)
14. I.J. Kim, B.C. Kim, C.Y. Yi, M. Shimizu, Y. Morishita, N. Saitoa, Bilateral comparison of the absorbed dose to water in high energy x-ray beams between the KRISS and the NMIJ. Nucl. Eng. Technol. **52**, 1511 (2020)
15. C. Thomas, The BIPM key comparison database (KCDB): linkage of key comparison results, Rapport BIPM-05/06, Bureau International des Poids et Mesures, Sèvres, France, 2005.
16. A.E. Walter and L.A. DeWerd, Evaluation of a Megavoltage Calibration Service at the Secondary Standard Level, 26th Annual Council of Ionization Radiation Measurements and Standards, April 16-18, 2018, National Institute of Standards and Technology, Gaithersburg, USA.
17. C.E. Andersen, G.V. Santurio, L. de Prez, On the potential of direct MV calibration of ionization chambers by secondary standard laboratories. Physica Media. **52**(Supplement 1), 11–12 (2018)
18. S.H. Kim, H. Huh, S.H. Choi, H.J. Kim, C. Lim, D.O. Shin, J. Choi, Chamber-to-chamber variation in the same type of a cylindrical chamber for the measurements of absorbed doses. Korean J. Med. Phys. **21**, 120–125 (2010)
19. I.J. Kim, B.C. Kim, J.H. Kim, J.P. Chung, H.M. Kim, C.-Y. Yi, Building a graphite calorimetry system for the dosimetry of therapeutic X-ray beams. Nucl. Eng. Technol. **49**, 810–816 (2017)

20. Y.H. Kim, C.Y. Yi, I.J. Kim, B.C. Kim, J.H. Kim, Y.M. Seong, H.M. Kim, Monte Carlo studies on dose conversion factors from graphite to water for high energy X-ray beams. Radiat. Phys. Chem. **171**, 108760 (2020)
21. G. Ramanathan, P. Harty, T. Wright, J. Lye, D. Butler, D. Webb., and R. Huntley, The Australian Primary Standard for Absorbed Dose to Water (Graphite Calorimeter), Technical Report No. 166, Australian Radiation Protection and Nuclear Safety Agency, 2014.
22. R.F. Nutbrown, S. Duane, D.R. Shipley, R.A.S. Thomas, Evaluation of factors to convert absorbed dose calibrations from graphite to water for the NPL high-energy photon calibration service. Phys. Med. Biol. **47**, 441–454 (2002)
23. Y. Morishita, M. Kato, N. Takata, T. Kurosawa, T. Tanaka, N. Saito, A standard for absorbed dose rate to water in a ^{60}Co field using a graphite calorimeter at the national metrology institute of Japan. Radiat. Prot. Dosim. **154**, 331–339 (2012)
24. I. Kawrakow, E. Mainegra-Hing, D.W.O. Rogers, F. Tessier, and B.R.B. Walters, 2015, The EGSnrc Code System: Monte Carlo simulation of electron and photon transport. Technical Report PIRS-701 (CNRC Canada).
25. B. Owen, A.R. DuSautoy, Correction for the effect of the gaps around the core of an absorbed dose graphite calorimeter in high energy photon radiation. Phys. Med. Biol. **36**, 1699–1704 (1991)
26. M.R. McEwen, A.R. DuSautoy, Primary standards of absorbed dose for electron beams. Metrologia **46**, S59–S79 (2009)
27. J. Renaud, A. Sarfehnia, J. Bancheri, J. Seuntjens, Aerrow: a probe-format graphite calorimeter for absolute dosimetry of high-energy photon beams in the clinical environment. Med. Phys. **45**, 414–428 (2018)
28. J. Witzani, K.E. Duftschmid, Ch. Strachotinsky, A. Leitner, A graphite absorbed-dose calorimeter in the quasi-isothermal mode of operation. Metrologia **20**, 73–79 (1984)
29. I.J. Kim et al., Thermal analysis of a graphite calorimeter for the measurement of megavoltage photon beam absorbed dose, 2014 APMP TCRI Workshop, Daejeon (2014).
30. J. Seuntjens, S. Duane, Photon absorbed dose standards. Metrologia **46**, S39–S58 (2009)
31. M.R. McEwen, A.R. DuSautoy, Primary standards of absorbed dose for electron beams. Metrologia **46**, S59–S79 (2009)
32. N.I. Kalach, D.W.O. Rogers, Which accelerator photon beams are "clinic-like" for reference dosimetry purposes? Med. Phys. **30**, 1546–1555 (2003)
33. Code of Practice for the Absorbed Dose Determination in High Energy Photon and Electron Beams, Report 18 of the Netherlands Commission on Radiation Dosimetry Revised edition, August 2012.
34. K.R. Shortt, C.K. Ross, M. Schneider, K. Hohlfeld, M. Roos, A.M. Perroche, A comparison of absorbed dose standards for high energy X-rays. Phys. Med. Biol. **38**, 1937–1955 (1993)
35. C.K. Ross, K.R. Shortt, D.W.O. Rogers, and F. Delaunay, A test of $TPR_{20,10}$ as a beam quality specifier for high energy photon beams, Measurement Assurance in Dosimetry (Proc. Symp. Vienna, 1993) IAEA, 309–321,1994.
36. A.S. Guerra, R.F. Laitano, M. Pimpinella, Experimental determination of the beam quality dependence factors, k_Q, for ionisation chambers used in photon and electron dosimetry. Phys. Med. Biol. **40**, 1177–1190 (1995)
37. H. Palmans, W. Mondelaers, H. Thierens, Absorbed dose beam quality correction factors k_Q for the NE2571 chamber in a 5 MV and a 10 MV photon beam. Phys. Med. Biol. **44**, 647–663 (1999)
38. J.P. Seuntjens, C.K. Ross, K.R. Shortt, D.W.O. Rogers, Absorbed-dose beam quality conversion factors for cylindrical chambers in high energy photon beams. Med. Phys. **27**, 2763–2779 (2000)
39. S. Duane, and M.H. Simon, Experimental determination of the quality-dependent correction factor k_Q for ionisation chambers of type NE2561, NE2611 and NE2571, Proceedings of the World Congress on Medical Physics and Biomedical Engineering, Aug 24–29, 2003, Sydney, Australia
40. J. Medin, C.K. Ross, N.V. Klassen, H. Palmans, E. Grusell, J.-E. Grindborg, Experimental determination of beam quality factors, k_Q, for two types of Farmer chamber in a 10 MV photon and a 175 MeV proton beam. Phys. Med. Biol. **51**, 1503–2152 (2006)
41. A. Krauss, R.-P. Kapsch, Calorimetric determination of k_Q factors for NE 2561 and NE 2571 ionization chambers in 5 cm×5 cm and 10 cm×10 cm radiotherapy beams of 8 MV and 16 MV photons. Phys. Med. Biol. **52**, 6243–6259 (2007)
42. M.R. McEwen, Measurement of ionization chamber absorbed dose k_Q factors in megavoltage photon beams. Med. Phys. **37**, 2179–2193 (2010)
43. L. de Prez, J. de Pooter, B. Jansen, T. Perik, F. Wittkämper, Comparison of kQ factors measured with a water calorimeter in flattening filter free (FFF) and conventional flattening filter (cFF) photon beams phys. Med. Bio. **63**, 045023 (2018)
44. E. Mainegra-Hing, B.R. Muir, On the impact of ICRU report 90 recommendations on k_Q factors for high-energy photon beams. Med. Phys. **45**, 3904–3908 (2018)
45. J. Tikkanen, K. Zink, M. Pimpinella, P. Teles, J. Borbinha, J. Ojala, T. Siiskonen, C. Gomà, M. Pinto, Calculated beam quality correction factors for ionization chambers in MV photon beams. Phys. Med. Biol. **65**, 075003 (2020)
46. D.M. González-Castaño, G.H. Hartmann, F. Sánchez-Doblado, F. Gómez, R.-P. Kapsch, J. Pena, R. Capote, The determination of beam quality correction factors: Monte Carlo simulations and measurements. Phys. Med. Biol. **54**, 4723–4741 (2009)

Publisher's Note Springer Nature remains neutral with regard to jurisdictional claims in published maps and institutional affiliations.

Springer Nature or its licensor holds exclusive rights to this article under a publishing agreement with the author(s) or other rightsholder(s); author self-archiving of the accepted manuscript version of this article is solely governed by the terms of such publishing agreement and applicable law.